Eur Biophys J (1998) 27: 403–408

BIOPHYSICS LETTER

Daniel Riveline · Albrecht Ott · Frank Jülicher
Donald A. Winkelmann · Olivier Cardoso
Jean-Jacques Lacapère · Soffia Magnúsdóttir
Jean-Louis Viovy · Laurence Gorre-Talini
Jacques Prost

Acting on actin: the electric motility assay

Received: 2 March 1998 / Accepted: 23 March 1998

Abstract We have developed a novel technique which allows one to direct the two dimensional motion of actin filaments on a myosin coated sheet using a weak electric field parallel to the plane of motion. The filament velocity can be increased or decreased, and even reversed, as a function of orientation and strength of the field. PMMA (poly(methylmethacrylate)) gratings, which act as rails for actin, allow one for the first time to explore three quadrants of the force velocity diagram. We discuss effective friction, duty ratio and stall force at different myosin densities. A discontinuity in the velocity force relationship suggests the existence of dynamical phase transition.

Key words Actin · Myosin · Electric fields · PMMA · Instability

Introduction

Actin-myosin motility assays (Kron and Spudich 1986; Kishino and Yanagida 1988; Toyoshima et al. 1990; Harada et al. 1990; Winkelmann et al. 1995) have become a standard tool to analyze members of this motor protein family in order to gain insight into the link between protein structure and mechanical behavior. Even if very interesting information has been obtained by measuring the speed of actin moving on a myosin sheet, full knowledge of the force velocity relationship is necessary for a complete characterization. The actin filament velocity can be reduced by increasing the frictional forces of the filament with respect to its environment (Warshaw et al. 1990; Janson et al. 1992; Haeberle and Hemric 1995); however, this approach does not allow for instantaneous modification of the applied load during the experiment and it only imposes forces opposing the direction of motion. Furthermore, accurate calibration of the force remains difficult. The behavior of individual molecular motors or collections of motors have been probed with microneedles (Kishino and Yanagida 1988; Ishijima et al. 1991; Ishijima et al. 1996) and optical tweezers (Svoboda et al. 1993; Kuo and Sheetz 1993; Finer et al. 1994, 1995; Molloy et al. 1995). These elegant but technicaly difficult approaches have yielded measurements of average stalling forces of the order of 1 pN, peak forces around 5 pN and elementary steps of about 5–20 nm produced by individual myosin molecules.

We have developed a novel approach to impose a versatile and easily controllable force on filaments by applying an electric field parallel to the plane of motion of the F-actin in an acto-myosin motility assay. The electric field exerts a mechanical force on the negatively charged actin filaments which increases or decreases the filament speed depending on the direction of motion with respect to the field. We present a study of the filament speed as a function of electric field strength and obtain the effective friction of the acto-myosin system and discuss it in relation to the myosin duty ratio. The stall force is measured and an instability near stalling conditions is revealed.

D. Riveline · A. Ott (✉) · F. Jülicher · J.-J. Lacapère
S. Magnúsdóttir · J. L. Viovy · L. Gorre-Talini · J. Prost
Laboratoire PhysicoChimie Curie (associé au Centre National de la Recherche Scientifique (CNRS) et à l'Université Paris 7), Institut Curie, Section de Recherche,
11 Rue Pierre et Marie Curie, F-75231 Paris Cedex 05, France

D. A. Winkelmann
Department of Pathology, Robert Wood Johnson Medical School, Piscataway, NJ 08854, USA

O. Cardoso
Laboratoire de Physique Statistique (associé au Centre National de la Recherche Scientifique (CNRS) et aux Universités Paris 6 et Paris 7), Ecole Normale Supérieure,
24 Rue Lhomond, F-75231 Paris Cedex 05, France

Experimental (Material and methods)

The actin filaments are manipulated with an external electrical field using the experimental setup depicted in Fig. 1. The motion of actin filaments was observed either on a flat myosin sheet, or it was constrained parallel to the field using a patterned substrate made of myosin coated

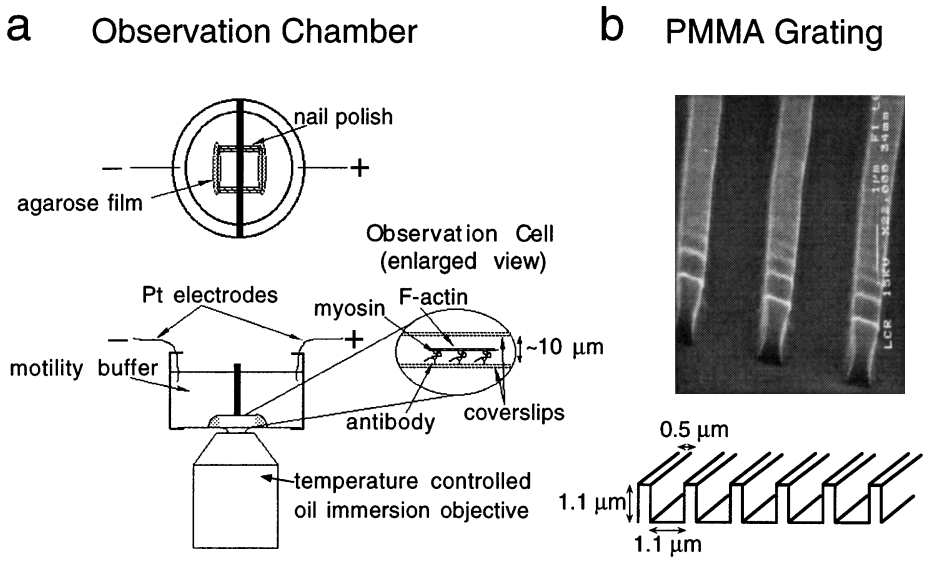

Fig. 1 **a** The observation chamber (home-built, scales are not respected): the motility assay is prepared according to Winkelman et al. (1995) on a round coverslip, 35 mm in diameter. It is covered with a squared 18×18 mm coverslip, previously incubated with 0.1% bovine serum albumin (A-3803, Sigma) in water and dried. Two opposite edges of the coverslip are sealed with Nail polish (Multi Eclat, Clarins), and along the remaining edges 1% agarose (A-6013, Sigma) in motility buffer is applied to avoid buffer drift and loss of actin. This cell is inserted into a Plexiglas chamber, divided into two reservoirs, each filled with 2 ml of motility assay buffer. The only electrical connection between the reservoirs is via the motility assay (see enlarged view). Platinum electrodes are inserted via holes in the two reservoirs. Temperature within the observation cell is controlled via the oil immersion objective which is kept at 30.0 °C. Variations of the electrophoretic mobility of free actin filaments are less than 10% across the depth of the cell, thus electrohydrodynamic flow generated by electroosmosis on the coated surfaces is negligible. **b** View by electron microscopy of PMMA gratings used as a substrate for the motility assay, dimensions below. These gratings were found to direct actin motion (courtesy of D. Adam and F. Champagne, Thomson CSF). Gratings were made to order by Thomson CSF, France

PMMA (poly(methylmethacrylate)) (Suzuki et al. 1997) using the antibody capture technique in both cases (Winkelmann et al. 1995). Motility assay buffer contained 7.5 mM MgATP. Experiments were performed at 30 °C . AC and DC fields were applied with a function generator followed by a power amplifier (7500, Krohn-Hite). The motility assay was observed with a temperature controlled 63× Plan Apochromat objective on an inverted microscope (Axiovert 100, Zeiss), equipped with epifluorescence optics, illuminated with a 100 W mercury light source and rhodamine filter sets. Neutral density filters were added to reduce illumination. Images were projected onto an image intensifier (C2400-80, Hamamatsu) coupled to a CCD camera (XC-77CE, Sony). Contrast and brightness were adjusted through a PCvision Frame Grabber driven with Optimas (Bioscan) software and images were recorded on S-VHS videotape. A green LED connected to the function generator was placed in the objective light path to signal inversion of the field polarity during observation. In order to measure filament speed video images were digitized with a Scion frame grabber and analysed with an interactive program tracking the leading edge of moving filaments. Coordinates of pointed ends of filaments with uninterrupted motion were taken typically every 0.1 s.

The electrophoretic mobility of rhodamine phalloidin labelled F-actin was measured in two ways: capillary electrophoresis in 100 µm fused silica capillaries (DB17-100 µm, J&W Scientific) yields a value of $\mu_B = 5.5 \cdot 10^{-9}$ m^2/Vs. Direct measurement of the mobility of filaments in bulk in the experimental setup yields $\mu_B = 1.0 \cdot 10^{-8}$ m^2/Vs. The latter value was chosen since conditions are indentical to the motility assay whereas sticking to the walls of the capillary might have influenced the measurement of the former.

Results and discussion

On applying the electrical field on a flat substrate the local interaction of the filament with the myosin motors appears unchanged, but the direction of filament motion orients along the electric field such that the negatively charged actin filaments are propelled toward the positive electrode (Fig. 2a,b). Filaments trapped by defects of the myosin surface can often be freed by the electric field. Upon field inversion, many of the filaments make U-turns apparently with their contour following the leading tip. For a saturated myosin surface of around 900 molecules/µm^2 the onset of visible orientation occurs for field strengths of around $5 \cdot 10^2$ V/m; above fields of $\approx 5 \cdot 10^3$ V/m motion against the field is rare.

The direction of filament motion can be confined by a patterned grating of 1 µm wide grooves photoetched into PMMA (Fig. 1b). The actin filaments move straight along the grooves occasionally changing to a neighboring track and this even when moving against an opposing electric field (Fig. 2c). Typical velocity distributions of F-actin moving on myosin at different field strengths are shown in

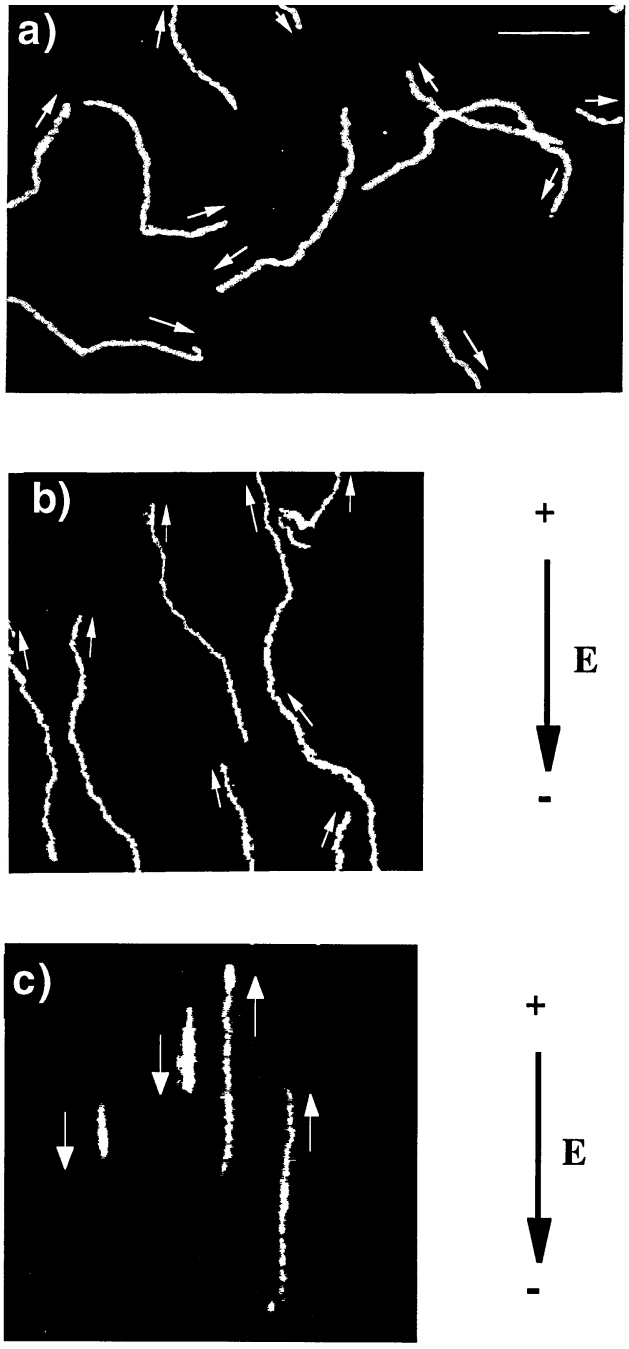

Fig. 2a–c Paths of actin filaments on a myosin coated surface, arrows indicate direction of motion. **a** In the absence of an electric field, directions of the filaments are uniformly distributed (myosin density of 900proteins/μm^2). **b** In the presence of an electric field of $2.5 \cdot 10^3$ V/m paths are oriented along the field direction. Moving tips of actin filaments are directed towards the negative electrode (myosin density of 900proteins/μm^2). **c** PMMA gratings as a substrate direct actin filament motion parallel to the grooves. An electric field of $3 \cdot 10^3$ V/m is applied parallel to the grooves (myosin density of 200 proteins/μm^2). Figures show an average of a few videoframes followed by thresholding to obtain a binary image. The length of the filaments is ≈4 μm. Note that, as a result of the velocity changes due to the presence of an electric field, paths are longer in (**b**) than in (**a**). In (**c**) the superimposed images of slow filaments moving towards the positive electrode appear to be shorter and thicker than for fast filaments moving in the opposite direction since the former have time to fluctuate within the groove. *Scale bar*, 10 μm

Table 1 The field to stall actin motion as a linear function of myosin density. The value for 900 proteins/μm^{-2} is not a direct measurement, but an extrapolation

Myosin density	100 μm^{-2}	200 μm^{-2}	400 μm^{-2}	900 μm^{-2}
Stall field (10^3 V/m)	–2.3±0.2	–5±1	–11±1	–17±2

Fig. 3. Those filaments moving towards the anode are faster than without an external field (Fig. 3a,b) and those moving in the opposite direction are slower. Most motion stops at the stall field strength, E_s which varies linearly with myosin surface density (Table 1). Interestingly, near stalling conditions, a subpopulation is observed representing about 10% of the total F-actin which continues to move; some of these filaments move forward at a slow speed and some move backwards (Fig. 3c). Many filaments in this subpopulation even reverse direction from time to time. With strong opposing fields, motion is reversed: the filaments move backward against their natural direction at a speed depending on field strength (Fig. 3d).

The field-velocity relationship has been investigated over a range of myosin surface densities spanning an order of magnitude (Fig. 4). At a low myosin density, around 100 molecules/μm^2, many filaments surprisingly keep their direction of motion even on a flat substrate when the field is reversed. In this case, the entire field-velocity relation can be obtained without the use of PMMA gratings. At surface densities above 200 molecules/μm^2 PMMA gratings have been used to prevent turning of the actin filaments when moving against the field. A linear velocity-field relationship of the form, $v = v_0 + \mu E$, holds for weak fields up to an absolute value of about $4 \cdot 10^3$ V/m, where v_0 is the spontaneous velocity and μ is and effective mobility coefficient. For stronger fields these curves appear increasingly concave. Near stalling conditions a discontinuity of the force velocity relationship is observed at myosin surface densities above 100 molecules/μm^2. Varying the field amplitude around the stall value while observing selected filaments revealed a hysteretical behavior i.e. switching between back and forward motion occurred for a continuously increasing and decreasing field at different values. It seems unlikely that this phenomenon is due to inhomogeneities of the myosin substrate since this unstable population only appears near stalling conditions (Fig. 3). We interpret this discontinuity of the force-velocity relationship as the signature of a dynamical phase transition of the acto-myosin system around zero speed. The possible existence of an instability of this type, resulting from a collective effect of many motors attached to a single filament, has been predicted by theoretical arguments based on a simple model (Jülicher and Prost 1995).

The mechanical force exerted by the field on the actin filament can be estimated as $f \approx \xi_h \mu_B E$, where μ_B is the electrophoretic mobility of actin measured in bulk solution and ξ_h is the hydrodynamic friction coefficient per unit length of a filament close to the surface. For ξ_h we use the expression of the friction of a rod near a wall $\xi_h \approx 2\pi\eta/\ln((D+(D^2-R^2)^{1/2})/R)$ (Hunt et al. 1994) with η

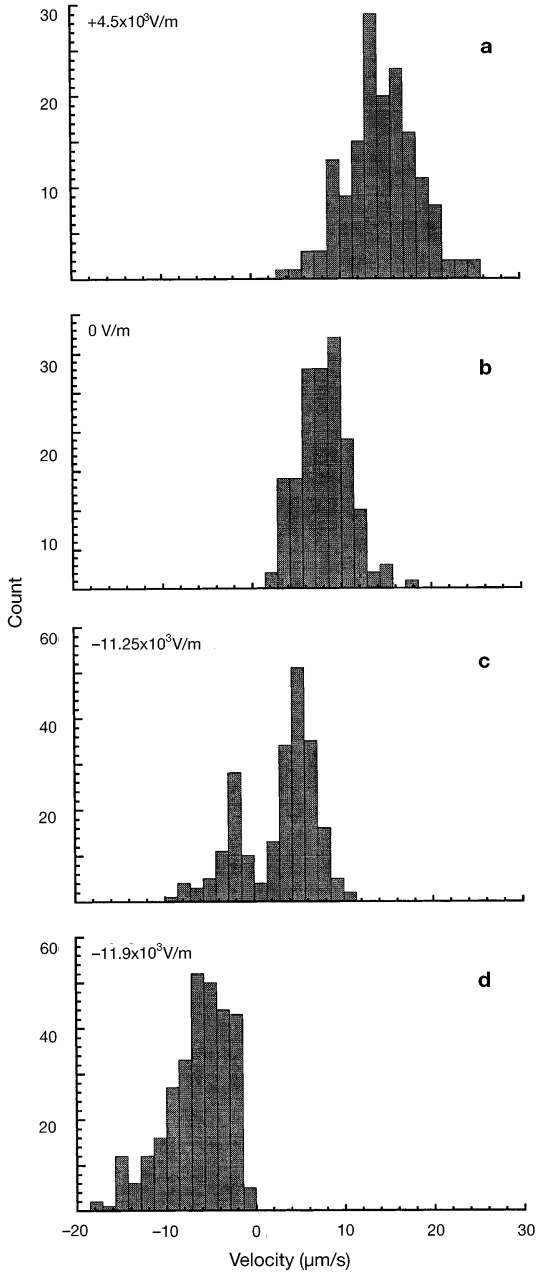

Fig. 3a–d Histograms of velocity distributions for a myosin density of 400/μm^2 for different values of the electric field. The field is applied parallel to the grooves of the PMMA grating which is used as a substrate for motility. Speeds of actin filaments moving towards the positive electrode **a** are increased compared to the natural speed distribution without an electric field depicted in **b**. Filaments moving towards the negative electrode are slowed down by the field (not shown). **c** For a strong opposing field around stalling value about 10% of the filaments are still moving, however backward and forward motion is observed. The two peaks of the histogram of the moving filaments reveal a discontinuity of the speed-force relation interpreted a signature of an instability of the actin-myosin motor. **d** Upon a small further increase of the field strength all filaments move backwards

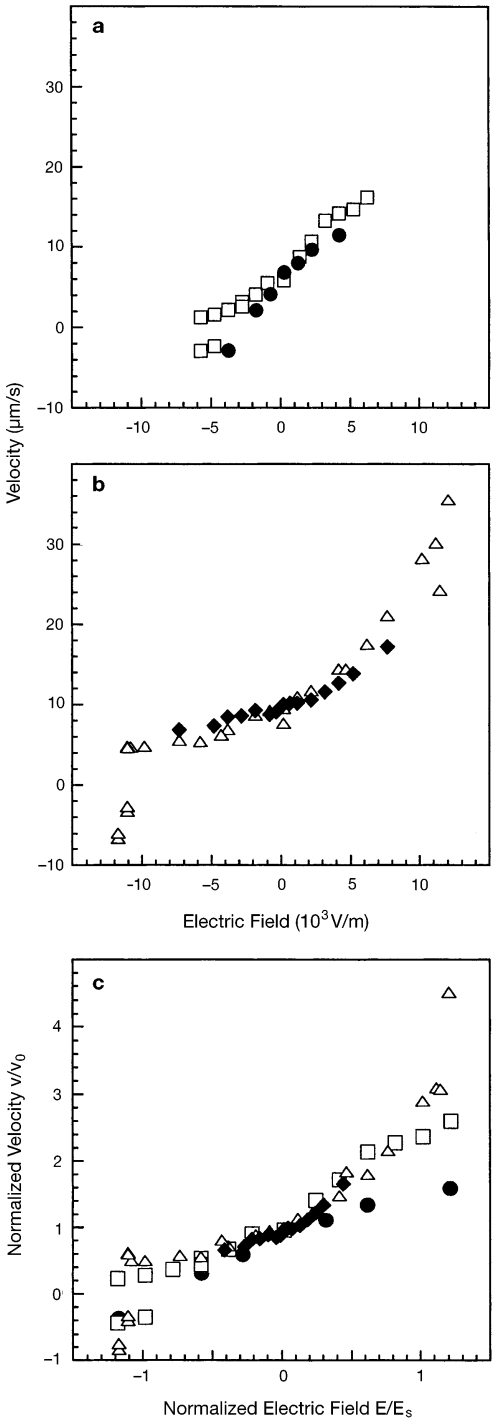

Fig. 4a–c Average velocity of actin filaments as a function of the electric field at T=30°C and 7.5 mM ATP in PMMA gratings. Only moving filaments were counted. The sign of the field is chosen with respect to actin motion: E>0 field causes acceleration, E<0 deceleration. Myosin densities are **a** 100 (circles) and 200 (squares), **b** 400 (triangles) and 900 (diamonds) proteins/μm^2. As shown in the histogram of Fig. 3 c, positive and negative speeds occur around the stall-field (surface densities of 200 and 400 proteins/μm^2) as a signature of an instability discussed in the text. **c** Our observations should not depend on the absolute value of the applied electric field but on the force per motor. The curves in (**a**) and (**b**) should be superposable after rescaling: the graph v/v_0 as a function of E/E_s (where v_0 is the velocity in absence of field and E_s is the stall field) shows that force-velocity diagrams have indeed a very similar shape for different myosin densities

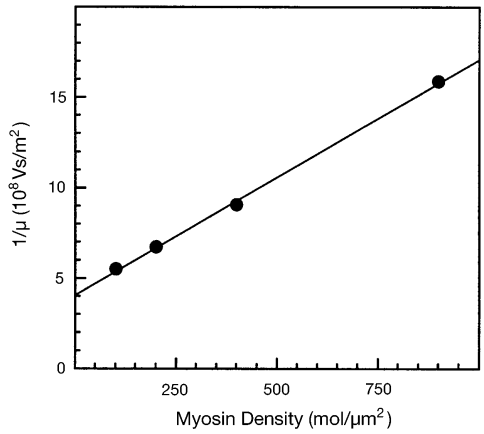

Fig. 5 The effective friction μ^{-1} of the actin myosin motor scales linearly with myosin surface density. Mobilities μ were obtained as the slope of the velocity-field diagrams for fields between $\pm 4 \cdot 10^3$ V/m. The straight line is a linear fit

denoting the solvent viscosity, R the filament radius and D the distance between the filament axis and the surface. Since the actin filament is expected to be at a molecular distance between filament and surface, we use $D/R \approx 1.1$, yielding $\xi_h \mu_B \approx 2 \cdot 10^{-10}$ N/V. The force per unit length acting on a filament is $f \approx 2$ pN/μm for electrical fields of 10^4 V/m.

The fact that the observed stall fields and hence the stall forces change linearly with myosin surface density σ (Table 1) supports the assumption that the number of myosin heads, n, interacting per unit length with the filament is given by $n = \sigma a$, where $a \approx 30$ nm is the reach of a motor. Using this value, we obtain an average force per myosin head of 0.15 pN which is similar to 0.2 pN reported by Kishino and Yanagida (1988) for a force acting at the extremity of the actin filament. The inverse of the mobility μ (taken as the slope of the field velocity relation $\mu = \Delta v/\Delta E$) is related to a friction coefficient $\xi \approx \Delta f/\Delta v = \xi_h \mu_B/\mu$, which describes the velocity increase, Δv, resulting from an externally applied force per length, Δf. for weak fields this friction scales linearly with myosin density (Fig. 5). At high myosin density μ^{-1} is about an order of magnitude larger than the value extrapolated to zero myosin density, $\mu_s^{-1} = 4 \cdot 10^8$ Vs/m^2. This value is about 4 times larger than $1/\mu_B$ in bulk, indicating a contribution of non-hydrodynamic friction due to the proximity of actin to the surface.

Assuming that the weak binding state contributes to friction of the order of ξ_h, the effective friction ξ is caused mainly by myosin heads in the strong binding state. A simple argument relates the observed actin mobility to the duty ratio. The external force induces an elastic displacement $\delta = (\ell/c)\,\Delta f$ of the actin filament segment of length ℓ, defined by the distance between two strongly bound myosin, with c^{-1} denoting the combined longitudinal elasticity of actin filament and acto-myosin crossbridge in units of force/length. This displacement leads to a velocity increase $\Delta v \approx \delta/\tau$, where $\tau \approx 2 \cdot 10^{-3}$ s is the 'strongly bound state time' (Spudich 1994), and the friction coefficient can thus be expressed as $\xi = \tau c/\ell$. The average distance of motors $d = 1/(a\,\sigma)$ along the filament, can be related to ℓ by $\ell \approx d/r$, where r denotes the acto-myosin duty ratio. If the dominant displacement δ arises from the elasticity of the acto-myosin crossbridge (Tawada and Sekimoto 1991; Leibler and Huse 1993) $r \approx \xi d/(c\tau)$; using $d \approx 30$ nm for $\sigma = 900$ μm^{-2} and the observed friction $\xi = 0.30$ Ns/m^2 and taking $c \approx 1.3 \cdot 10^{-4}$ N/m (Molloy 1995) we estimate $r \approx 0.05$. If the dominant contribution to the displacement arises from actin filament bending deformations, we can estimate $c \approx \pi^4 \kappa^2/(\ell^4\,kT)$ for a filament with bending rigidity κ at temperature T and Boltzmann constant k. Using $\kappa/kT \approx 10$ μm we obtain a similar estimate for the duty ratio as previously, $r \approx (\xi\,kT\,d^5/(\pi^4\tau^2\tau))^{1/5} = 0.04$. Taking into account that both, myosin crossbridge- and actin filament elasticity, contribute simultaneously, we estimate $r \approx 0.05$. Note that longer times τ would correspond to even smaller duty ratios. Using this estimate of 5% of the duty ratio, we obtain a force during power stroke of 3 pN per myosin, which agrees well with earlier measurements of the mean force during power stroke (Kishino and Yanagida 1988; Ishijima et al. 1991, 1996; Finer et al. 1994, 1995; Molloy et al. 1995; Bourdieu et al. 1995).

Besides exerting a force on actin, electric fields might interfere in multiple ways with actin-myosin. Indeed, fields of large amplitude led to a noticeable increase in temperature of the assay. Electric fields could in principle also influence the cycle of ATP hydrolysis or they could orient or deform myosin molecules. Deformation of myosin has been suggested for electric fields of an order of magnitude larger than those we have used; see e.g. (Highsmith and Eden 1986). These effects should then depend on the frequency for AC fields and should therefore lead to frequency dependent velocities. We applied to the motility assay alternating rectangular signals with zero-mean amplitude with frequencies between 100 Hz and 10 kHz that were both symmetric and asymmetric with respect to time. A frequency independent increase of velocity due to heating of the sample was observed for AC field amplitudes comparable to those used with DC fields. At a field of $4 \cdot 10^3$ V/m heating was expected to account for less than 25% of the observed velocity increase.

In conclusion, we show that weak electric fields corresponding to millivolts across micrometers provide a novel and simple tool for manipulating actin filaments in motility assays and for exerting piconewton forces homogeneously distributed along the filaments. The linearity of the velocity change versus the external field for amplitudes below $4 \cdot 10^3$ V/m allows one to gain information on the effective friction of the motor and to estimate its duty ratio. We confirm the smallness of the duty ratio at high ATP concentration. We further measure directly the stall force and analyze the behavior of the actin myosin system under stalling conditions: for myosin densities above 200 proteins/μm^2, our data suggests the existence of a hysteretical discontinuity in the speed-velocity relation. It is interesting to note that experiments on single muscle fibers show anomalies around zero speed (Edman 1988) or oscillations under appropriate conditions (Yasuda 1996), com-

patible with the above described instability (Jülicher and Prost 1997). Further experiments are clearly needed to exactly pin down its nature; exploration of the phase diagram should be very helpful in this respect.

Acknowledgements We are grateful to Bernard Clergeaud and Danile Lévy for stimulating help. We thank Olivier Thoumine, Michel Bornens, and Daniel Louvard for fruitful discussions. One of us (J. P.) is very grateful to S. Ishiwata for pointing out Edman (1988) and Yasuda et al. (1996), and to K. Kinoshita for sending us unpublished data compatible with the idea of an instability. He further acknowledges illuminating discussions with both of them. This work was supported by grants from Institut Curie and the USPHS grant AR38454 to D. A. Winklemann.

References

Bourdieu L, Duke T, Elowitz MB, Winkelmann DA, Leibler, Libchaber A (1995) Spiral defects in motility assays: a measure of motor protein force. Phys Rev Lett 75: 176–179

Edman KA (1988) Double-Hyperbolic nature of the force velocity relation in frog skeletal muscle. Ad Exp Med Biol 226: 643–652

Finer JT, Simmons RM, Spudich JA (1994) Single myosin molecule mechanics: piconewton forces and nanometer steps. Nature 368: 113–119

Finer JT, Mehta AD, Spudich JA (1995) Characterization of single actin-myosin interactions. Biophys 68: 291s–297s

Haeberle JR, Hemric ME (1995) Are actin filaments moving under unloaded conditions in the in vitro motility assay? Biophys J 68: 306s–311s

Harda Y, Sakurada K, Aoki T, Thomas DD, Yanagida T (1990) Mechanomechanical coupling in actomyosin energy transduction studied by in vitro movement assay. J Mol Biol 216: 49–68

Highsmith S, Eden D (1986) Myosin subfragment 1 has tertiary structural domains. Biochem 25: 2237–2242

Hunt AJ, Gittes F, Howard J (1994) The force exerted by a single kinesin molecule against a viscous load. Biophys J 67: 766–781

Ishijima A, Doi T, Sakurada K, Yanagida T (1991) Sub-piconewton force fluctuations of actomyosin in vitro. Nature 352: 301–306

Ishijima A, Kojima H, Higuchi H, Harada Y, Funatsu T, Yanagida T (1996) Multiple- and single-molecule analysis of the actomyosin motor by nonometer-piconewton manipulation with a microneedle: unitary steps and forces. Biophys J 70: 383–400

Janson LW, Sellers JR, Taylor DL (1992) Actin-binding proteins regulate the work performed by myosin II motors on single actin filaments. Cell Motil Cytoskelet 22: 274–280

Jülicher F, Prost J (1995) Cooperative molecular motors. Phys Rev Lett 75: 2618–2621

Jülicher F, Prost J (1997) Spontaneous oscillations of collective molecular motors. Phys Rev Lett 78: 4510–4513

Kishino A, Yanagida T (1988) Force measurements by micromanipulation of a single actin filament by glass needles. Nature 334: 74–76

Kuo SC, Sheets MP (1993) Force of single kinesin molecules measured with optical tweezers. Science 250: 232–234

Kron SJ, Spudich J (1986) Fluorescent actin filaments move on myosin fixed to a glass surface. Proc Natl Acad Sci USA 83: 6272–6276

Leibler S, Huse DA (1993) Porters versus rowers: a unified stochastic model of motor proteins. J Cell Biol 121: 1357–1368

Molloy JE, Burns JE, Sparrow JC, Tregear RT, Kendrick-Jones J, White DCS (1995) Single-molecule mechanics of heavy meromyosin and S1 interacting with rabbit or drosophila actins using optical tweezers. Biophys J 68: 298s–305s

Spudich JA (1994) How molecular motors work. Nature 372: 515–518

Suzuki H, Yamada A, Oiwa K, Nakayama H, Mashiko S (1997) Control of actin moving trajectory by patterned poly(methylmethacrylate) tracks. Biophys J 72: 1997–2001

Svoboda K, Schmidt CF, Schnapp BJ, Block SM (1993) Direct observation of kinesin stepping by optical trapping interferometry. Nature 365: 721–727

Tawada K, Sekimoto K (1991) A physical model of ATP-induced actin-myosin movement in vitro. Biophys J 59: 343–356

Toyoshima YY, Kron SJ, Spudich JA (1990) The myosin step size: measurement of the unit displacement per ATP hydrolyzed in an in vitro assay. Proc Natl Acad Sci USA 87: 7130–7134

Warshaw DM, Desrosiers JM, Work SS, Trybus KM (1990) Smooth muscle myosin cross-bridge interactions modulate actin filament sliding velocity in vitro. J Cell Biol 111: 453–463

Winkelmann DA, Bourdieu L, Ott A, Kinose F, Libchaber A (1995) The flexibility of myosin attachment to surfaces influences F-Actin motion. Biophys J 68: 2444–2453

Yasuda K, Shindo Y, Ishiwata S (1996) Synchronous behaviour of spontaneous oscillations of sarcomeres in skeletal myofibrils under isotonic conditions. Biophys J 70: 1823–1829